Received: 13 January 2022 | Accepted: 26 June 2022

DOI: 10.1111/1751-7915.14115

RESEARCH ARTICLE

microbial biotechnology Open Access

GATA transcription factor WC2 regulates the biosynthesis of astaxanthin in yeast *Xanthophyllomyces dendrorhous*

Ruilin Huang[1,2] | **Ruirui Ding**[2,3] | **Yu Liu**[2,3] | **Fuli Li**[2,3] | **Zhaohui Zhang**[1] | **Shi'an Wang**[2,3]

[1]College of Food Science and Engineering, Ocean University of China, Qingdao, China

[2]Shandong Provincial Key Laboratory of Synthetic Biology, Chinese Academy of Sciences, Qingdao Institute of Bioenergy and Bioprocess Technology, Qingdao, China

[3]Shandong Energy Institute, Qingdao, China

Correspondence

Zhaohui Zhang, College of Food Science and Engineering, Ocean University of China, Qingdao 266100, China.
Email: zhangzhh@ouc.edu.cn

Shi'an Wang, Shandong Provincial Key Laboratory of Synthetic Biology, Qingdao Institute of Bioenergy and Bioprocess Technology, Chinese Academy of Sciences, Qingdao 266101, China.
Email: wangsa@qibebt.ac.cn

Funding information
National key Research and Development Program of China, Grant/Award Number: 2018YFE0107200; National Natural Science Foundation of China, Grant/Award Number: 51861145103 and 31670054; Shandong Energy Institute, Grant/Award Number: SEI I202136

Abstract

Astaxanthin is a type of carotenoid widely used as powerful antioxidant and colourant in aquaculture and the poultry industry. Production of astaxanthin by yeast *Xanthophyllomyces dendrorhous* has attracted increasing attention due to high cell density and low requirements of water and land compared to photoautotrophic algae. Currently, the regulatory mechanisms of astaxanthin synthesis in *X. dendrorhous* remain obscure. In this study, we obtained a yellow *X. dendrorhous* mutant by Atmospheric and Room Temperature Plasma (ARTP) mutagenesis and sequenced its genome. We then identified a putative GATA transcription factor, white collar 2 (XdWC2), from the comparative genome data and verified that disruption of the *XdWC2* gene resulted in a similar carotenoid profile to that of the ARTP mutant. Furthermore, transcriptomic analysis and yeast one-hybrid (Y1H) assay showed that XdWC2 regulated the expression of phytoene desaturase gene *CrtI* and astaxanthin synthase gene *CrtS*. The yeast two-hybrid (Y2H) assay demonstrated that XdWC2 interacted with white collar 1 (XdWC1) forming a heterodimer WC complex (WCC) to regulate the expression of *CrtI* and *CrtS*. Increase of the transcriptional levels of *XdWC2* or *CrtS* in the wild-type strain did not largely modify the carotenoid profile, indicating translational and/or post-translational regulations involved in the biosynthesis of astaxanthin. Overexpression of *CrtI* in both the wild-type strain and the *XdWC2*-disrupted strain apparently improved the production of monocyclic carotenoid 3-hydroxy-3′, 4′-didehydro-β, ψ-carotene-4-one (HDCO) rather than β-carotene and astaxanthin. The regulation of carotenoid biosynthesis by XdWC2 presented here provides the foundation for further understanding the global regulation of astaxanthin biosynthesis and guides the construction of astaxanthin over-producing strains.

Ruilin Huang and Ruirui Ding authors contributed equally to this work.

INTRODUCTION

Carotenoids are a group of tetraterpenoids with increasing applications as feed additives, nutraceuticals, cosmetics and pharmaceuticals (Martínez-Cámara et al., 2021). Nowadays, more than 750 carotenoid types have been described from natural sources and about 50 carotenoids are components of the human nutrition (Barreiro & Barredo, 2018). Some carotenoids have been commercialized, such as lycopene, β-carotene, zeaxanthin, astaxanthin and fucoxanthin (Bogacz-Radomska & Harasym, 2018; Liang et al., 2019; Mohamadnia et al., 2020; Zafar et al., 2021). Among them, astaxanthin (3, 3′-dihydroxy-β, β'-carotene-4, 4′-dione) exhibits strong antioxidant activities (Naguib, 2000; Shimidzu et al., 1996), as well as anti-inflammatory, cardioprotective and hepatoprotective activities (Fakhri et al., 2018; Mussagy et al., 2021).

Astaxanthin has been commercially used as a nutritional supplement for human and a feed colourant in aquaculture and the poultry industry (Stachowiak & Szulc, 2021). It is mainly produced by the yeast *Xanthophyllomyces dendrorhous* (anamorph *Phaffia rhodozyma*) in the form of (3*R*, 3′*R*) and the algae *Haematococcus pluvialis* in the form of (3*S*, 3′*S*) (Ambati et al., 2014). The (3*R*, 3′*R*)-isomer from *X. dendrorhous* was usually used in aquaculture and the poultry industry, while the (3*S*, 3′*S*)-isomer from *H. pluvialis* was mainly used for human consumption (Basiony et al., 2022; Moretti et al., 2006). Both (3*S*, 3′*S*) and (3*R*, 3′*R*) stereoisomers can be efficiently absorbed by the human body (Rüfer et al., 2008). It was reported that the global astaxanthin market size reached $1.37 billion in 2020 and was forecasted to $4.75 billion of revenue in 2028. Aquaculture and animal feeds account for more than 47% of the global market share (Grand View Research, Inc., 2021).

The biosynthetic pathway of astaxanthin has been established in *X. dendrorhous* (Figure 1) (Rodríguez-Sáiz et al., 2010). In brief, isopentenyl pyrophosphate (IPP) is synthesized via the mevalonate (MVA) pathway and isomerized to dimethylallyl pyrophosphate (DMAPP) by IPP isomerase, and then geranylgeranyl pyrophosphate (GGPP) is yielded by farnesyl pyrophosphate synthase (FPPS) and GGPP synthase CrtE. Two molecules of GGPP are linked by the bifunctional enzyme CrtYB (phytoene synthase and lycopene cyclase) to form phytoene. Lycopene and γ-carotene are synthesized sequentially under the catalysis of phytoene desaturase CrtI and CrtYB. γ-Carotene can be converted into bicyclic carotenoid β-carotene and monocyclic carotenoid torulene via the enzymes CrtYB and CrtI, respectively. Next, β-Carotene is converted to astaxanthin by the astaxanthin synthase CrtS and cytochrome P450 reductase CrtR. Torulene is used as the substrate to synthesize 3-hydroxy-3′, 4′-didehydro-β, ψ-carotene-4-one (HDCO) (Barredo et al., 2017; Torres-Haro et al., 2021). Obviously, multifunctional enzymes and switch pathways are involved in astaxanthin biosynthesis in *X. dendrorhous*, exhibiting the complexity of the regulatory processes.

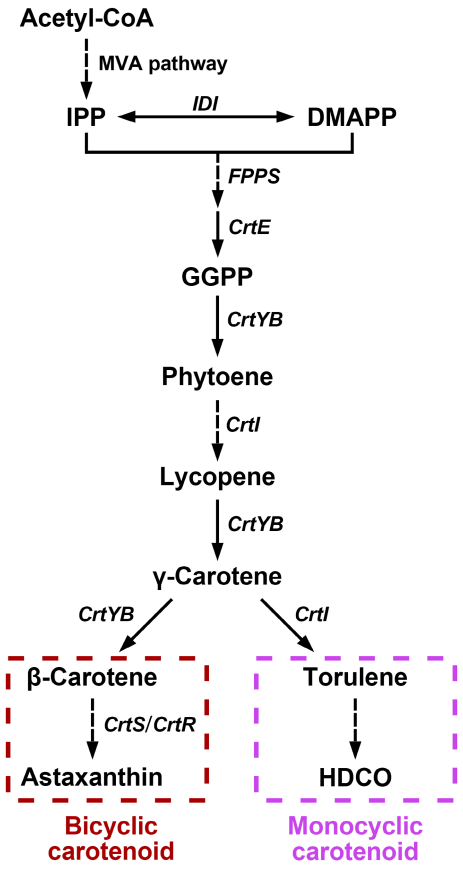

FIGURE 1 The pathway of carotenoid biosynthesis in *X. dendrorhous*. MVA, mevalonate; IPP, isopentenyl pyrophosphate; DMAPP, dimethylallyl pyrophosphate; GGPP, geranylgeranyl pyrophosphate; HDCO, 3-hydroxy-3′, 4′-didehydro-β, ψ-carotene-4-one. *IDI*, IPP delta isomerase gene; *CrtE*, GGPP synthase gene; *CrtI*, phytoene desaturase gene; *CrtYB*, phytoene synthase gene or lycopene cyclase gene; *CrtS*, astaxanthin synthase gene; *CrtR*, cytochrome P450 reductase gene.

The sterol regulatory element-binding protein 1 (Sre1) regulates the biosynthesis of both sterol and carotenoid in *X. dendrorhous* (Gómez et al., 2020). Sre1 is a transcription factor boosting the transcriptional expression of genes *CrtE* and *CrtR* in the carotenoid pathway (Gómez et al., 2020, 2021). The expression of genes *CrtI*, *CrtYB* and *CrtS* is repressed by the zinc finger protein MIG1 in high-sugar cultures (Wozniak et al., 2011). However, the regulatory mechanisms of astaxanthin synthesis in *X. dendrorhous* remain further investigation. In this study, we performed ARTP mutagenesis on the *X. dendrorhous* wild-type strain CBS 6938 to identify astaxanthin-producing mutants and investigated the genetic variations related to astaxanthin biosynthesis by forward genetics in a mutant M1-3RC. The genome of M1-3RC was sequenced and a putative GATA transcription factor was identified from

comparative genome data. Disruption of the GATA gene in the wild-type strain resulted in a similar carotenoid profile to that of the ARTP mutant, suggesting that the putative GATA transcription factor regulates the biosynthesis of astaxanthin. This study verified the GATA transcription factor and investigated its roles in carotenoid biosynthesis by transcriptomic analysis, the Y1H assay, the Y2H assay and genetic engineering.

EXPERIMENTAL PROCEDURES

Strains and culture conditions

The cultivation of yeast strains was performed according to a previous study with minor modification (Zhang et al., 2019). *X. dendrorhous* strains used in this study are listed in Table 1. The liquid YPD medium (2% glucose, 2% peptone and 1% yeast extract) was used for standard cultivation. The liquid YM medium (2% glucose, 0.5% peptone, 0.3% yeast extract and 0.3% malt extract) was used for production of carotenoid. Yeast strains were inoculated into 25 ml of liquid medium in 250-ml flasks and cultivated at 22°C with 250 rpm of rotary shaking in incubators.

Plasmid construction

All the plasmids used in this study were constructed by Gibson assembly method according to a previous study (Zhang et al., 2019). In brief, DNA fragments amplified by KAPA HiFi Hotstart ReadMix (Roche) were assembled at 50°C for 1 h by using 2× Pro Ligation-Free Cloning MasterMix (Applied Biological Materials Inc.). Primers used in this study were described in File S4. The plasmids constructed in this study were listed in Table 1.

To construct the plasmid pDevc, the promoter P_{TEF} in pUG6 was replaced by the promoter of glucose dehydrogenase gene (P_{GDH}) that was amplified from the genomic DNA (gDNA) of *X. dendrorhous* CBS 6938 using a primer pair Devc-PgdhF/PgdhR. The backbone DNA fragment of pDevc was amplified from the plasmid pUG6 using a primer pair Devc-BF/BR. To generate pDevc-xdwc2, two homologous arms flanking *XdWC2* were amplified from the gDNA of CBS 6938 using primer pairs of TF-upF/upR and TF-dnF/dnR, and backbone fragments were amplified from the plasmid pDevc using primer pairs TF-smF/smR and TF-vcF/vcR. To construct the plasmid pB42AD-XdWC2, coding sequence (CDS) of *XdWC2* was amplified from the cDNA of CBS 6938 using a primer pair XdG-F/R, and backbone DNA was amplified from the plasmid pB42AD (pJG4-5) using a primer pair pJGG-F1/R1. To generate the plasmid pLacZi2μ-pCrtS, promoter of *CrtS* was amplified from gDNA of CBS 6938 using a primer pair pCS-nF/nR, and backbone DNA was amplified from the plasmid pLacZi2μ using a primer pair pLZI-nF/nR. To construct the plasmids pGBKT7-XdWC2 and pGADT7-XdWC1, CDS of *XdWC2* and *XdWC1* were amplified from the cDNA of CBS 6938 using primer pairs GBD-CDS-F/R and WC1AD-WC1-F/R, respectively. Backbone DNA fragments used in constructing pGBKT7-XdWC2 was amplified from the plasmid pGBKT7 using primer pairs GBD-B1-F/R and GBD-B2-F/R. Backbone DNA fragments used in constructing pGADT7-XdWC1 was amplified from the plasmid pGADT7 AD using primer pairs WC1AD-B1-F/R and WC1AD-B2-F/R.

Electroporation of *X. dendrorhous*

Electroporation of *X. dendrorhous* was performed according to a previous publication (Wery et al., 1998). Briefly, cells were incubated in freshly made 25 mM of DTT potassium phosphate buffer at room temperature and resuspended in ice-cold STM buffer (270 mM of sucrose, 10 mM of Tris–HCl of pH 7.5, 1 mM of $MgCl_2$) to make competent cells. Approximately 10 μg DNA fragments were mixed with competent cells, loaded into 2 -mm pulser cuvettes and electroporated by BTX ECM 630 (Genetronics) at 1000 Ω, 800 V and 50 μF. Transformants were selected on YPD plates supplemented with 200 μg/ml of G418, Zeocin or Hygromycin B.

Extraction of total RNA from *X. dendrorhous*

Strains grown for 2 days in YPD medium were inoculated into YM medium and cultivated continuously. The cultures were separately harvested at growing for 24, 28 and 120 h, and 1 ml of each culture was centrifugated. Next, the supernatant was discarded and the cell samples were frozen in liquid nitrogen and then cryopreserved at −80°C or immediately used. RNA extraction was performed by using the Rapid RNA Extraction Kit (Tianmo Biotech, China), according to the manufacturer's application protocol. Yeast cells were broken using 0.5 -mm glass beads (Omega Bio-Tek) with the help of a FastPrep-24™ (MP biomedicals) instrument. The mixture of cells and glass beads was vigorously vibrated at 6.0 m/s for 40 s and the process was repeated for four times.

ARTP mutagenesis

The *X. dendrorhous* strain CBS 6938 was grown in YPD medium until OD_{600} reached 1 to 1.4. ARTP mutagenesis was carried out on an ARTP instrument (Wuxi Tmaxtree Biotechnology Co., Ltd.). Helium was used as

TABLE 1 Strains and plasmids used in this study

Strain and plasmid	Genotype or description	Source
X. dendrorhous		
CBS 6938	Wild-type	CBS collection
M1-3RC	ARTP mutant	This study
Xd-wc2	*xdwc2::G418*^{R}	This study
Xd-Cwc2	*xdwc2::G418*^{R}, *rDNA::(XdWC2 + Zeocin*^{R})	This study
Xd-rDL-WC2	*rDNA::(XdWC2 + Zeocin*^{R})	This study
Xd-wc1	*xdwc1::G418*^{R}	This study
Xd-cryD	*cryD::G418*^{R}	This study
Xd-aif	*aif::G418*^{R}	This study
Xd-acp	*acp::G418*^{R}	This study
Xd-clp1	*clp1::G418*^{R}	This study
Xd-cnh	*cnh::G418*^{R}	This study
Xd-rho	*rho::G418*^{R}	This study
Xd-gh3	*gh3::G418*^{R}	This study
Xd-abcT	*abcT::G418*^{R}	This study
Xd-cry	*cry::G418*^{R}	This study
Xd-bluF	*bluF::G418*^{R}	This study
Xd-wc2-CI	*xdwc2::G418*^{R}, *rDNA::(CrtI + HGR*^{R})	This study
Xd-wc2-CS	*xdwc2::G418*^{R}, *rDNA::(CrtS + HGR*^{R})	This study
Xd-wc2-CIS	*xdwc2::G418*^{R}, *rDNA::(CrtS-CrtI + HGR*^{R})	This study
Xd-CI	*rDNA::(CrtI + HGR*^{R})	This study
Xd-CS	*rDNA::(CrtS + HGR*^{R})	This study
Xd -CIS	*rDNA::(CrtS-CrtI + HGR*^{R})	This study
Saccharomyces cerevisiae		
EGY48	Y1H assay strain, MATα type	AngYuBio LC.
AH109	Y2H assay strain, MATα type	AngYuBio LC.
Plasmids		
pUG6	Backbone vector, G418^R	EUROSCARF
pDevc	Derived from pUG6, P_{GDH}	This study
pDevc-xdwc2	For the disruption of *XdWC2*, G418^R	This study
pDevc-xdwc1	For the disruption of *XdWC1*, G418^R	This study
pDevc-cryD	For the disruption of *CryD*, G418^R	This study
pDevc-aif	For the disruption of *Aif*, G418^R	This study
pDevc-acp	For the disruption of *ACP*, G418^R	This study
pDevc-clp1	For the disruption of *Clp1*, G418^R	This study
pDevc-cnh	For the disruption of *CNH*, G418^R	This study
pDevc-rho	For the disruption of *Rho*, G418^R	This study
pDevc-abcT	For the disruption of *AbcT*, G418^R	This study
pDevc-cry	For the disruption of *Cry*, G418^R	This study
pDevc-bluF	For the disruption of *BluF*, G418^R	This study
pDevc-gh3	For the disruption of *GH3*, G418^R	This study
pUG6-rDL	Containing rDNA homologous arms	Zhang et al. (2019)
pUG6-rDL-XdWC2	*rDNA::*P_{GPD}*-XdWC2-*T_{Actin}, Zeocin^R	This study
pUG6-rDL-CI	*rDNA::*P_{ADH4}*-CrtI-*T_{GPD}, Hgr^R	This study
pUG6-rDL-CS	*rDNA::*P_{ADH4}*-CrtS-*T_{GPD}, Hgr^R	This study
pUG6-rDL-CIS	*rDNA::*P_{ADH4}*-CrtS-*T_{GPD}*-*P_{ADH4}*-CrtI-*T_{GPD}, Hgr^R	This study

(Continues)

TABLE 1 (Continued)

Strain and plasmid	Genotype or description	Source
pB42AD (pJG4-5)	Backbone vector, carrying *B42 AD* and *TRP1*	Clontech Laboratories Inc.
pB42AD-XdWC2	*B42 AD-XdWC2*, *TRP1*	This study
pLacZi2μ	Backbone vector, carrying *LacZ* and *URA3*	Lin et al. (2007)
pLacZi2μ-pActin	P_{Actin}-P_{CYC1}-*LacZ*, *URA3*	This study
pLacZi2μ-pCrtS	P_{CrtS}-P_{CYC1}-*LacZ*, *URA3*	This study
pLacZi2μ-pCrtI	P_{CrtI}-P_{CYC1}-*LacZ*, *URA3*	This study
pGADT7 AD	Backbone vector, carrying *GAL4 AD* and *LEU2*	Clontech Laboratories Inc.
pGADT7-T	Positive control in Y2H	Clontech Laboratories Inc.
pGADT7-XdWC1	*GAL4 AD-XdWC1*, *LEU2*	This study
pGBKT7	Backbone vector, carrying *GAL4 BD* and *TRP1*	Clontech Laboratories Inc.
pGBKT7-53	Positive control in Y2H	Clontech Laboratories Inc.
pGBKT7-XdWC2	*GAL4 BD-XdWC2*, *TRP1*	This study

working gas at 10 L/min. The power input of the ARTP system was 115 W at a driving frequency of 13.56 MHz. The distance between the plasma torch nozzle and the sample was set as 2 mm and a plasma jet temperature of 30°C was used. An aliquot (10 μl) of cell culture was loaded onto an iron plate, and exposed to ARTP irradiation for different time periods at 30, 60, 120, 180, 210 and 240 s. The treated cells were harvested and re-suspended in distilled water. The cell suspension was diluted, spread on high C/N YM agar plates (6% glucose, 0.5% peptone, 0.3% yeast extract and 0.3% malt extract), and incubated at 22°C for 5 days. Cell lethal rate was calculated according to the number of the colonies of the irradiated strains and controls growing on YM plates.

Genome resequencing

The genome sequences of the ARTP mutants were sequenced by Illumina technique. Standard genome sequencing and standard bioinformatic analyses were provided by Oebiotech. The sequence reads were filtered by fastp version 0.20.1 based on a Q-score threshold of 20 (Chen et al., 2018). Clean reads account for 99.5% of raw reads (1.41 G of clean bases vs. 1.42 G of raw bases) in the sequencing data of M1-3RC. Clean reads were mapped to the reference genome *X. dendrorhous* rsharma.33.13 (EMBL: ERR575093-ERR575095) using the BWA 0.7.16a software (Li & Durbin, 2009). The duplicate reads were removed by Picard version 2.7.2 after file format conversion by SAMtools (Li et al., 2009). The mean coverage of the genome data of M1-3RC was 49.3-fold and the mean mapping quality score was 48.1. The GATK4 HaplotypeCaller was used to detect SNPs and Indels according to a threshold value of 2.0 for QD value (McKenna et al., 2010). Raw read sequencing data has been deposited in the NCBI database under the accession number PRJNA751450.

Sequence and structure analysis of GATA transcription factors

Conserved domains of XdWC2 were recognized by InterPro (http://www.ebi.ac.uk/interpro/) (Blum et al., 2021) and NCBI Batch CD-search (Yang, Derbyshire, et al., 2020a). The motif distribution of WC2 was analysed by online MEME tool version 5.4.1 (https://meme-suite.org/meme/tools/meme) (Bailey et al., 2009), using the following parameters: a minimum width of 10, a maximum width of 60, a motif number of 10, one occurrence per sequence (oops) and other default parameters. Motif distribution was depicted by using TBtools v1.098661 (Chen et al., 2020).

The phylogenetic analysis of GATAs was performed by ClustalX 2.1. Protein sequences of GATAs were downloaded from the GenBank database and compared using multiple alignment with a gap opening penalty of 10 and a gap extension penalty of 0.2. The phylogenetic tree was draw by the neighbour-joining method and the NJ plot using 1000 bootstrapped replicates (Larkin et al., 2007; Perrière & Gouy, 1996).

Transcriptomic analysis

RNA sequencing and standard bioinformatic analyses were provided by Oebiotech (Shanghai, China). In brief,

cDNA library was verified by Agilent 2100 Bioanalyzer (Agilent Technologies) and the Illumina HiSeq X Ten (Illumina) platform was used for sequencing to generate 125 or 150 bp paired data. Clean reads were aligned to the reference genome using hisat2 (Kim et al., 2015), and expression levels of coding genes were calculated by fragments per kb per million reads (FPKM) method (Roberts et al., 2011). GO and KEGG pathway enrichment analysis were performed according to standard methods. Raw read sequencing data has been deposited in the NCBI database under the accession number PRJNA752711.

qRT-PCR

The reverse transcription reaction of total RNA was performed by using the kit 5X All-In-One RT MasterMix with AccuRT (Applied Biological Materials Inc.) following the manufacturer's protocol. The qRT-PCR reaction consisted of 10 μl of MonAmp™ SYBR Green® qPCR Mix (Monad Biotech Co., Ltd.), 0.3 μM of each primer, 40 ng of cDNA and nuclease-free H_2O to a final volume of 20 μl. The amplification was carried out on a LightCycler 480 II (Roche) instrument. The amplification condition consisted of a pre-incubation at 95°C for 30 s, and 40 cycles of 95°C for 10 s and 60°C for 30 s. Next, the melting curve was obtained by heating at 95°C for 5 s, cooling at 55°C for 1 min, and then raising the temperature to 95°C at a ramp rate of 0.11°C/s. Primer pairs used in qRT-PCR were designed by Primer Premier 6 and the specificity of them were evaluated according to melting curves (File S4). The $2^{-\Delta\Delta CT}$ method was used to calculate the relative expression of genes (Livak & Schmittgen, 2001).

Yeast Y1H and Y2H assays

The Y1H assay was performed as previously described (Yang et al., 2020b) with some modifications. Briefly, the CDS of *XdWC2* was assembled into pB42AD (pJG4-5) by Gibson assembly to generate the prey plasmid pB42AD-XdWC2 for expressing the fusion protein containing B42 AD and XdWC2. Promoters of *CrtI*, *CrtS* and *Actin* genes were fused to the reporter gene *LacZ* in pLacZi2u to produce the bait-reporter plasmids pLacZi2μ-pActin, pLacZi2μ-pCrtS and pLacZi2μ-pCrtI, respectively. The prey plasmid and each of the bait-reporter plasmids were co-transformed into the *Saccharomyces cerevisiae* strain EGY48 (AngYu Biotechnologies Co., Ltd). Colonies were cultivated on SD/-Ura/–Trp plates. Next, positive colonies were assayed on the SD/-Ura/–Trp medium supplemented with 0.33% (v/v) X-gal, 1.25% (w/v) D-raffinose, 2.5% (w/v) galactose, and 10% (v/v) of 10×BU salts (3.9% $NaH_2PO_4{\cdot}2H_2O$ and 3.71% Na_2HPO_4, pH 7.0).

The Y2H assay was performed according to a previously study (Meng et al., 2018) with some modifications. Briefly, the CDSs of *XdWC2* and *XdWC1* were assembled into the vectors pGBKT7 and pGADT7 AD for expressing fusion proteins GAL4 BD-XdWC2 and GAL4 AD-XdWC1, respectively. The plasmids pGBKT7-53 and pGADT7-T were used as positive controls. The plasmids of BD series and AD series were correspondingly co-transformed into the *S. cerevisiae* strain AH109 (AngYu Biotechnologies Co., Ltd). Colonies were cultivated on SD/–Leu/–Trp plates, and then positive colonies were assayed on the SD/–Leu/–Trp/-His/–Ade plates for protein–protein interaction analysis.

Carotenoid extraction and detection

The carotenoid extraction procedure was adapted from a previous study with some modifications (Zhang et al., 2019). Briefly, 1 ml of cells were collected and washed by using 1 ml of deionized water. Cell sediment was then resuspended in 3 ml of dimethyl sulfoxide (DMSO) and incubated at 60°C for 2 h. The supernatant was collected after centrifugation. Next, 2 ml of acetone, 2 ml of petroleum ether and 2 ml of NaCl (20%, w/v) were added to the supernatant sequentially, mixed vigorously and centrifugated at 4000 *g* for 10 min to obtain carotenoid extracts. Carotenoid extracts were dried through nitrogen blowing and then dissolved in acetone.

HPLC was performed according to a previous protocol (Niklitschek et al., 2012) by using 1260 Infinity II LC System (Agilent Technologies, Inc.) equipped with a diode-array detector through a C_{18} column Poroshell 120 EC-C18 (4.6×150 mm, 4 μm) (Agilent Technologies, Inc.). Mobile phase consisted of acetonitrile/methanol/isopropyl alcohol (85:10:5, v/v/v). Samples were analysed at a flow rate of 1.0 ml/min. β-carotene, astaxanthin and HDCO were detected at 453, 474 and 494 nm, respectively. Concentrations of astaxanthin at 2×10^{-2}, 1×10^{-2}, 5×10^{-3} and 1×10^{-4} g/L were used to make the standard curve for astaxanthin, and concentrations of β-carotene at 2.3×10^{-2}, 1.15×10^{-2}, 2.875×10^{-3} and 5.75×10^{-4} g/L were used to make the standard curve for β-carotene.

Thin-layer chromatography (TLC) was performed as previously described (Chi et al., 2015). Carotenoids extracts were isolated on TLC silica gel 60 F_{254} (Merck KGaA) using the developing solvent consisting of acetone and *n*-hexane with a volume ratio of 3:7. The TLC was run until the distance between the solvent front and the baseline reaching 80 mm. The retention factor (Rf) was calculated according to the ratio between the travel distance of the tested compounds and that of the solvent front from the baseline. The Rf of astaxanthin achieved in this study was 0.26 and that of β-carotene was 0.88. The standard astaxanthin was purchased

from Shanghai Acmec Biochemical Co. Ltd and the standard β-carotene was from Shanghai Macklin Biochemical Co. Ltd.

RESULT

Genome resequencing of a yellow mutant

To obtain astaxanthin-producing mutants, we performed ARTP mutagenesis on the wild-type strain CBS 6938 using the radiation dosages with lethal rates between 80% and 95% (Figure 2A). A yellow mutant strain M1-3RC was acquired by two rounds of ARTP mutagenesis (Figure 2B). Its astaxanthin content decreased by 86%, while the β-carotene content increased 2.9-fold relative to CBS 6938 (377.8 vs. 129.5 μg/g) (Figure 2C).

We then adopted genome resequencing to detect genetic variations in M1-3RC. In total, 1179 single-nucleotide polymorphisms (SNPs) and 235 indels were identified (File S1), from which we identified six varied genes with amino acids changes, namely, transposon-encoded proteins CDZ96932.1 and CED85420.1, retrovirus-related gag-pol polyprotein CDZ97702.1, retrotransposon ty1-copia subclass CDZ97703.1, β-1,6-N-acetylglucosaminyltransferase CDZ97839.1 and a putative GATA transcription factor CDZ96439.1. We deduced that the mutation of CDZ96439.1 led to the change of astaxanthin production. A 'TG' inserted at the coding sequence of CDZ96439.1 resulting in a nonsense mutation and a truncation of the protein from a size of 619 amino acids (AAs) to 537 AAs (Figure 2D). Next, we analysed the sequence structure of CDZ96439.1. The results showed that the putative GATA transcription factor contained a typical PAS (Per-Arnt-Sim) domain and a C-X_2-C-X_{18}-C-X_2-C type GATA zinc-finger domain (Figure 2E), demonstrating that it is a member of the GATA family. The stop mutation (site 538) located in the GATA zinc finger (from site 536 to 561) and therefore led to the truncated protein losing DNA-binding capacity (Figure 2E).

Phylogenetic analysis of GATA transcription factors in fungi showed eight clades, including the previously identified families siderophore-regulating protein (SRP, Clade II), WC1 (Clade III), NsdD (Clade V) and WC2 (Clades VI and VII) (Park et al., 2006; Yu et al., 2019). CDZ96439.1 located in the clade of WC2 (Figure 3A). Comparative sequence analysis of WC2 proteins by the motif-based sequence analysis tool MEME suite exhibited 7 conserved motifs (Figure 3B). The motif 2, motif 3 and partial sequences of motif 1 located in the PAS domain. The size of CDZ96439.1 was apparently larger than the other WC2 proteins due to two longer linkers between motifs 3 and 4 and motifs 5 and 6 (Figure 3B). Although there were remarkable sequence differences in linkers, CDZ96439.1 had all the 7 conserved motifs. So, the GATA transcription factor CDZ96439.1 was entitled XdWC2 (*X. dendrorhous* WC2) in this study. Previous studies reported that WC2 proteins regulated the synthesis of carotenoids in fungi *Neurospora crassa* (Linden & Macino, 1997; Schmidhauser et al., 1994). Accordingly, XdWC2 probably regulates the biosynthesis of carotenoids in *X. dendrorhous* and this assumption has been further investigated.

Disruption and overexpression of *XdWC2*

The gene *XdWC2* was disrupted by inserting a geneticin-resistant gene via homologous recombination in the wild-type strain CBS 6938, generating a strain Xd-wc2. The astaxanthin content of Xd-wc2 decreased by 62% to 88 μg/g compared to 230 μg/g in CBS 6938 (Figure 4A). Meanwhile, the β-carotene content increased 4.7-fold to 474 μg/g relative to CBS 6938 (99.6 μg/g) (Figure 4A). The change of carotenoid production in Xd-wc2 was consistent with that in the mutant M1-3RC (Figure 2C), demonstrating a correlation between XdWC2 and the biosynthesis of both astaxanthin and β-carotene.

Next, we overexpressed the *XdWC2* gene in strains Xd-wc2 and CBS 6938, generating strains Xd-Cwc2 and Xd-rDL-WC2, respectively. The *XdWC2* gene was controlled by a constitutive promoter from the glucose-6-phosphate dehydrogenase (GPD)-encoding gene. The transcription of *XdWC2* were assayed by quantitative reverse transcription polymerase chain reaction (qRT-PCR) and carotenoid production was detected by high-performance liquid chromatography (HPLC). Although the expression of *XdWC2* in both Xd-Cwc2 and Xd-rDL-WC2 improved more than twenty-fold (Figure 4B), the content of astaxanthin and β-carotene was similar to the wild-type strain CBS 6938 (Figure 4A), indicating that translational and/or posttranslational regulations are involved in carotenoid biosynthesis in *X. dendrorhous*.

Transcriptomic analysis of the *XdWC2*-disrupted strain

To identify target genes of the transcription factor XdWC2, we sequenced the transcriptomes of the *XdWC2*-disrupted strain Xd-wc2 and the *XdWC2*-overexpressed strain Xd-rDL-WC2 when cultivated for 24 and 28 h, respectively. The time points were chosen due to a markable change in pigment production between Xd-wc2 and Xd-rDL-WC2 when cultivated for over 24 h (Figure 5A). Comparative transcriptome analysis identified 442 and 481 differentially expressed genes (DEGs) (fold change ≥2, $p \leq 0.05$) from the 24 and 28 h data set, respectively (Figure 5B, C). Further statistical analysis showed that there were 264 overlapping DEGs between the 24 and 28 h data set, consisting of 187

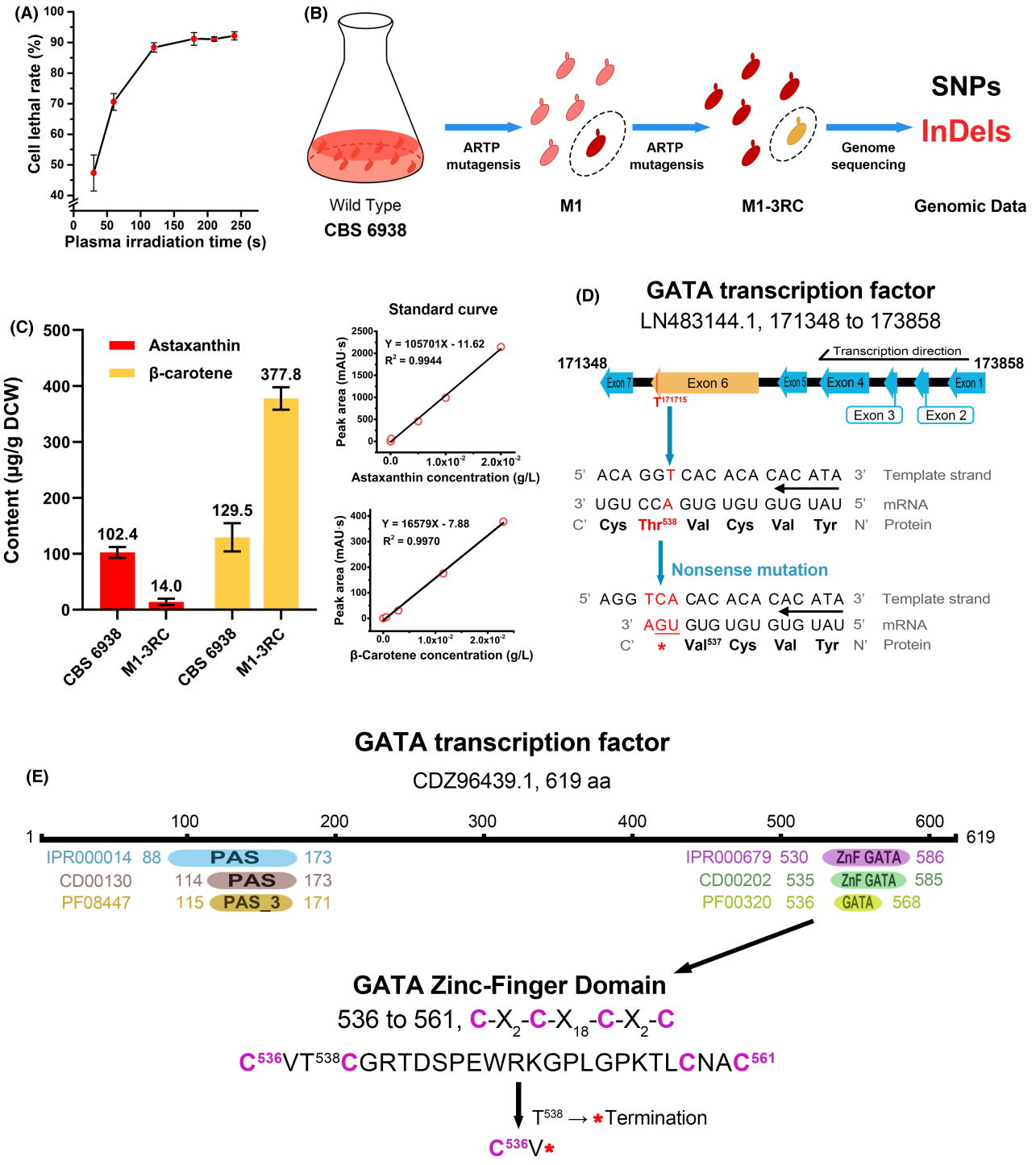

FIGURE 2 Identification of the GATA transcription factor. (A) The cell lethal rate of CBS 6938 in ARTP mutagenesis. (B) Flowchart for the ARTP mutagenesis of *X. dendrorhous*. M1 denotes a red mutant obtained in the first round of irradiation and M1-3RC denotes the yellow mutant obtained in the second round of irradiation. (C) The production of astaxanthin and β-carotene in the ARTP mutant M1-3RC and the control CBS 6938. (D) The 'TG' insertion in the gene of the putative GATA transcription factor CDZ96439.1. LN483144.1 denotes the sequence Scaffold_54 in GenBank database. (E) Sequence analysis showing the typical PAS (Per-Arnt-Sim) domain and a C-X_2-C-X_{18}-C-X_2-C type GATA zinc-finger domain in CDZ96439.1. The 'TG' insertion located in the GATA zinc-finger domain.

downregulated and 77 upregulated genes (Figure 5D, and File S2). Next, the overlapping DEGs were analysed by Gene Ontology (GO) term enrichment and Kyoto Encyclopedia of Genes and Genomes (KEGG) pathway analysis. GO enrichment analysis revealed that the DEGs were mainly enriched in GO terms: rRNA primary transcript binding, oxidoreductase activity and nucleolus (Figure 5E). KEGG pathway analysis showed that the DEGs were mainly involved in tryptophan metabolism, novobiocin biosynthesis, cyanoamino acid

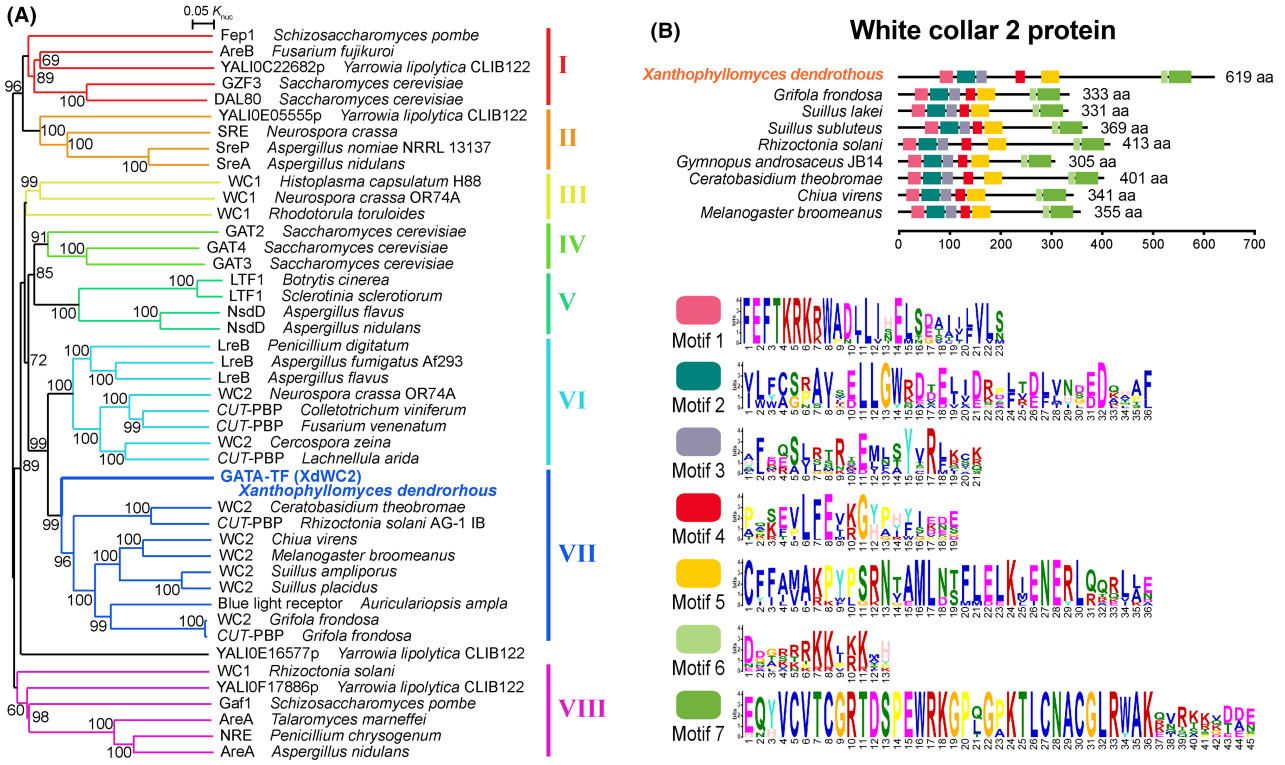

FIGURE 3 Comparative sequence analysis of GATA transcription factors. (A) A phylogenetic tree of GATA transcription factors in fungi constructed by ClustalX 2.1 using neighbour-joining method with 1000 bootstrapped replicates. (B) Comparative analysis of WC2 proteins by MEME suite exhibiting 7 conserved motifs. The sequences were derived from GenBank according to the accession numbers BAO20283 (*Grifola frondose*), KAG1754311 (*Suillus lakei*), KAG1891459 (*Suillus subluteus*), CUA69058 (*Rhizoctonia solani*), KAE9395386 (*Gymnopus androsaceus* JB14), KAB5596254 (*Ceratobasidium theobromae*), KAG9318635 (*Chiua virens*) and KAF9246368 (*Melanogaster broomeanus*).

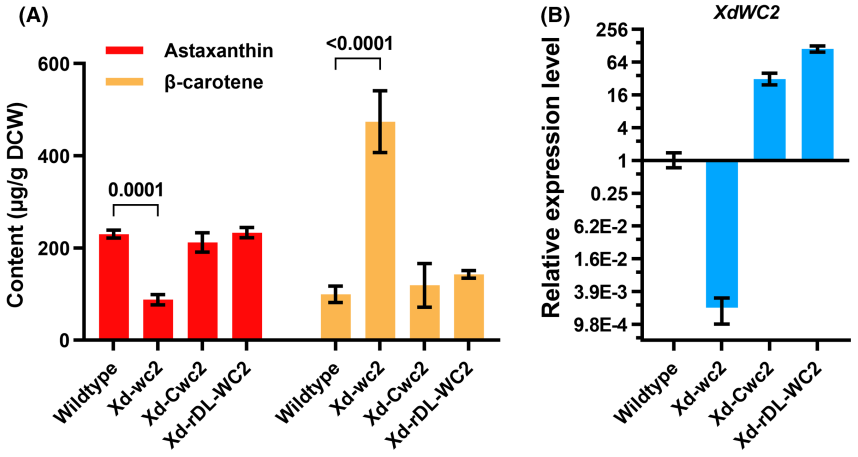

FIGURE 4 Expression of *XdWC2* influencing the biosynthesis of carotenoid. (A) The production of astaxanthin and β-carotene detected by HPLC. Wildtype, the strain CBS 6938; Xd-wc2, disrupting *XdWC2* in CBS 6938; Xd-Cwc2, restoring *XdWC2* at the native locus in Xd-wc2; Xd-rDL-WC2, overexpressing *XdWC2* at rDNA loci in Xd-wc2. (B) Expression of *XdWC2* assayed by qRT-PCR in the wild-type strain CBS 6938, and the recombinant strains Xd-wc2, Xd-Cwc2 and Xd-rDL-WC2 when cultivated for 120 h.

metabolism, glyoxylate metabolism and carotenoid biosynthesis (Figure 5F).

The biosynthesis of carotenoid in *X. dendrorhous* is strongly affected by nutrition sources (Marcoleta et al., 2011; Pan et al., 2017; Wang et al., 2019; Wozniak et al., 2011) and the FAD cofactor of phytoene dehydrogenase (Schaub et al., 2012). Accordingly, the DEGs encoding an apoptosis-inducing factor (AIF), a carbon-nitrogen hydrolase (CNH), an acid phosphatase (ACP) and a putative clampless 1 protein (Clp1) were analysed in addition to the DEGs *CrtI* and *CrtS* in the carotenoid pathway.

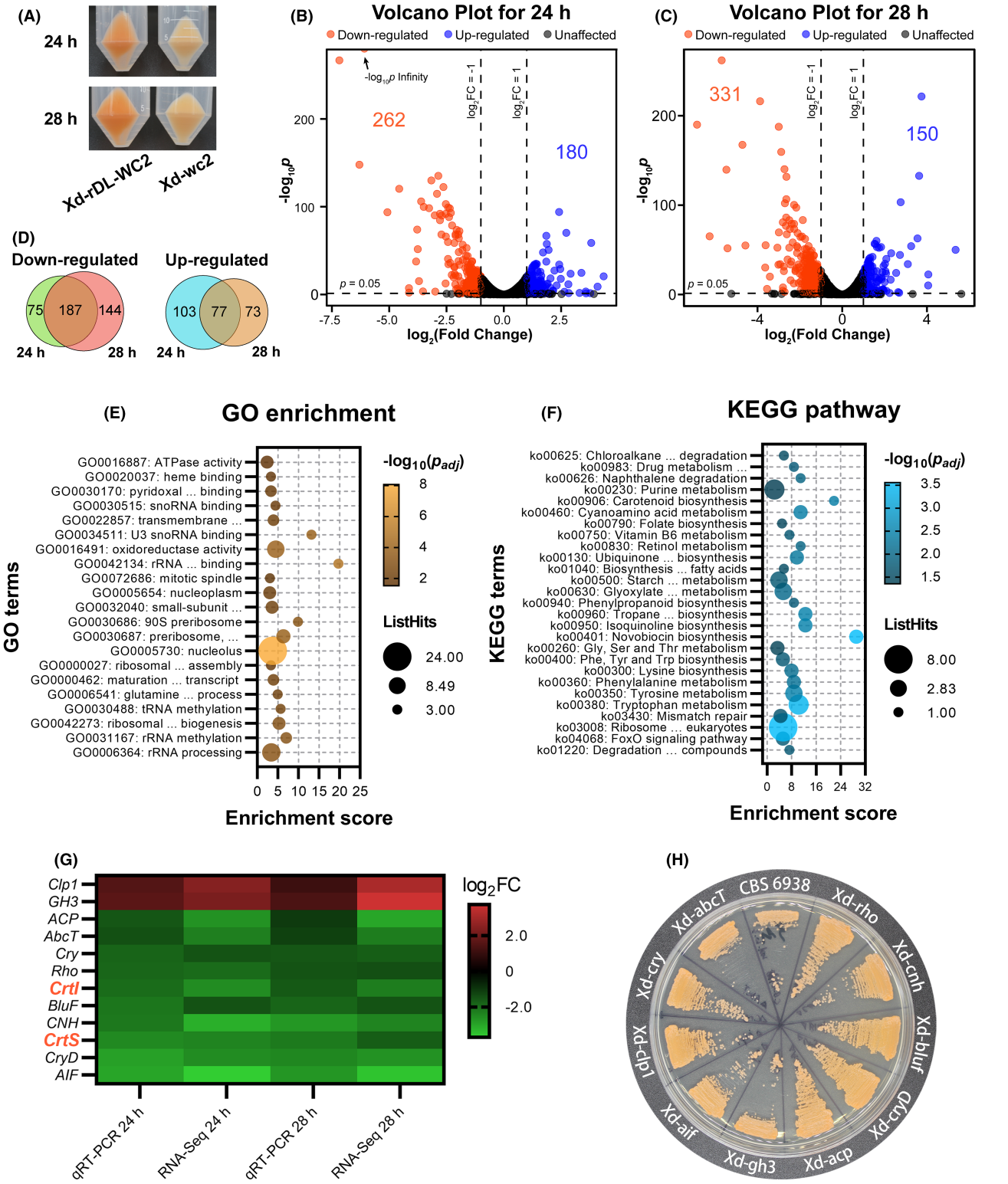

FIGURE 5 Transcriptomic analysis of the *XdWC2*-disrupted strain Xd-wc2 and the *XdWC2*-overexpressed strain Xd-rDL-WC2. (A) Comparison of the pigment in strains Xd-rDL-WC2 and Xd-wc2 cultivated in 50 ml liquid YM medium for 24 and 28 h. (B) and (C) Volcano plots of gene expression of the cultures growing for 24 h (B) and 28 h (C). (D) Venn plot of down-regulated and up-regulated differentially expressed genes (DEGs). (E) Gene Ontology term enrichment of overlapping DEGs between the 24 h data set and 28 h data set. (F) KEGG pathway analysis of overlapping DEGs between the 24 h data set and 28 h data set. (G) Comparison between the transcriptomic data and the qRT-PCR assay of the 12 selected genes. Clp1, Hypothetical protein; GH3, Glycoside hydrolase family 3 protein; ACP, Acid phosphatase; AbcT, ATP-dependent transporter; Cry, Cryptochrome; Rho, Rhodopsin; BLUF, BLUF domain protein; CNH, Carbon-nitrogen hydrolase; CryD, Cryptochrome DASH; AIF, Apoptosis-inducing factor. (H) The growth phenotype of the gene-disrupted strains cultivated on YM plates.

Considering possible evolutionary conservation of photoreactive proteins in the regulation of carotenoid biosynthesis, the DEGs encoding rhodopsin (Rho), cryptochrome (Cry), cryptochrome DASH (CryD) and BLUF-domain protein (BLUF) were also included in next analysis. Furthermore, the DEGs with over four-fold transcriptional changes at both 24 and 28 h data sets were recognized and the genes encoding an ATP-binding cassette (ABC) transporter (AbcT) and a glycoside hydrolase family 3 protein (GH3) were further investigated (File S3). Overall, 12 DEGs identified by comparative transcriptome analysis were validated by qRT-PCR (Figure 5G). It is clear that the genes *CrtI* and *CrtS* directly catalyse carotenoid synthesis (Álvarez et al., 2006). We then separately disrupted the 10 remaining DEGs to identify new regulators on the biosynthesis of carotenoid. Nevertheless, none of the mutants showed apparent phenotypic change (Figure 5H). Accordingly, *CrtI* and *CrtS* were supposed to be the targets directly regulated by XdWC2.

Detecting interaction of XdWC2 with *CrtI* and *CrtS*

The Y1H assay was used to detect interactions between XdWC2 and the promoters of *CrtI* and *CrtS*. XdWC2 was fused with the B42 activation domain (B42-AD). The reporter gene *LacZ* was driven by promoters P_{CrtI}, P_{CrtS} and P_{Actin} (control). Galactose induction showed that the *LacZ* controlled by P_{CrtI} or P_{CrtS} was obviously activated in contrast to the control, confirming the direct interaction of XdWC2 with the promoters of *CrtI* and *CrtS* (Figure 6A). Overexpression of *XdWC2* improved the expression levels of both *CrtI* and *CrtS* (Figure 6B), also supporting the regulation of *XdWC2* on the two genes.

To further evaluate the correlation between XdWC2 and the expression of *CrtI* and *CrtS*, we constructed a series of gene-overexpressed strains by using the constitutive strong promoter of alcohol dehydrogenase 4 (P_{ADH4}) and homologous recombination at the rRNA gene loci (Table 1). The genes *CrtI* and *CrtS* were separately overexpressed in CBS 6938 and Xd-wc2, producing strains Xd-CI, Xd-CS, Xd-wc2-CI and Xd-wc2-CS. Co-overexpressing *CrtI* and *CrtS* in CBS 6938 and Xd-wc2 generated strains Xd-CIS and Xd-wc2-CIS, respectively. The relative expression level of *CrtI* and *CrtS* was increased in all the overexpressed strains according to the qRT-PCR assay (Figure 6C, D). The production of carotenoid was analysed by HPLC and thin-layer chromatography (TLC) (Figure 6E, F). Because we did not acquire the standard compound of HDCO, HDCO was confirmed according to the comparison between the carotenoid profiles in TLC and HPLC based on a previous study (Figure 6E, F) (Chi et al., 2015).

We then measured the production of HDCO in strains CBS 6938, Xd-wc2, Xd-Cwc2 and Xd-rDL-WC2. Compared to CBS 6938, Xd-wc2 showed a decrease in the content of HDCO by 73%, whereas the strains Xd-Cwc2 and Xd-rDL-WC2 represented a HDCO content of 3.3-fold and 3.8-fold higher than Xd-wc2, respectively (Figure 6G). These data indicated that overexpression of *XdWC2* led to the increase of HDCO production in *X. dendrorhous*.

The HDCO content in Xd-CI and Xd-CIS increased 2.7-fold and 4-fold compared to that in CBS 6938, respectively (Figure 6H). While the content of β-carotene decreased by 75% to 25 μg/g from 100 μg/g along with an increase of HDCO in Xd-CIS (Figure 6H). Production of astaxanthin was not significantly modified by overexpression of *CrtI* and/or *CrtS* in strains Xd-CIS, Xd-CI and Xd-CS (Figure 6H) that was consistent to overexpressing *XdWC2* in CBS 6938, hinting a rigid regulation in astaxanthin biosynthesis in *X. dendrorhous*.

Overexpression of *CrtI* resulted in a 4.4-fold increase in HDCO content along with a 28% reduction of β-carotene content (342 vs. 474 μg/g) in Xd-wc2-CI and a 4.8-fold increase in HDCO content along with an 85% reduction of β-carotene content (70.5 vs. 474 μg/g) in Xd-wc2-CIS (Figure 6I). The content of astaxanthin was improved 1.83-fold to 161 μg/g in Xd-wc2-CS and 1.76-fold to 155 μg/g in Xd-wc2-CIS compared to Xd-wc2 (Figure 6I). These data indicated that the carotenoid profile in XdWC2-disrupted strains can be restored to similar fractions like in the wild-type strain overexpressing both *CrtI* and *CrtS*.

FIGURE 6 Detection of the interaction between *XdWC2* and genes *CrtI* and *CrtS*. (A) Interactions between XdWC2 and the promoters of *CrtI* and *CrtS* detected by the Y1H assay. (B) The expression of *CrtI* and *CrtS* assayed by qRT-PCR in the wild-type strain CBS 6938, and the recombinant strains Xd-Cwc2 and Xd-rDL-WC2 when cultivated for 120 h. (C) Gene expression of *CrtI* and *CrtS* assayed by qRT-PCR in wild-type strain CBS 6938, and the recombinant strains Xd-wc2, Xd-wc2-CI, Xd-wc2-CS and Xd-wc2-CIS when cultivated for 120 h. (D) Gene expression of *CrtI* and *CrtS* assayed by qRT-PCR in the wild-type strain CBS 6938, and the recombinant strains Xd-CI, Xd-CS and Xd-CIS when cultivated for 120 h. (E) Comparison of the carotenoid production between the wildtype strain CBS 6938 and the *CrtI* overexpressing strain Xd-CI detected by HPLC. The peaks at 6.53 and 6.56 min denote the predicted HDCO. The content of HDCO in Xd-CI is 2.75-fold of that in CBS 6938. (F) Determination of HDCO by the TLC assay referring to a previous study (Chi et al., 2015). 1, astaxanthin; 2, HDCO; 3 and 4, keto derivatives; 5, β-carotene. (G) Relative content of HDCO in the wild-type strain, Xd-wc2, Xd-Cwc2 and Xd-rDL-WC2. The peak area per 10 mg dry cells weight (mAU·s/10 mg DCW) was used to denote the relative content of HDCO. (H) The content of β-carotene, astaxanthin and HDCO detected by HPLC in the wild-type strain CBS 6938, Xd-CI, Xd-CS and Xd-CIS when cultivated for 120 h. (I) The content of β-carotene, astaxanthin, and HDCO detected by HPLC in the wild-type strain, Xd-wc2, Xd-wc2-CI, Xd-wc2-CS and Xd-wc2-CIS when cultivated for 120 h.

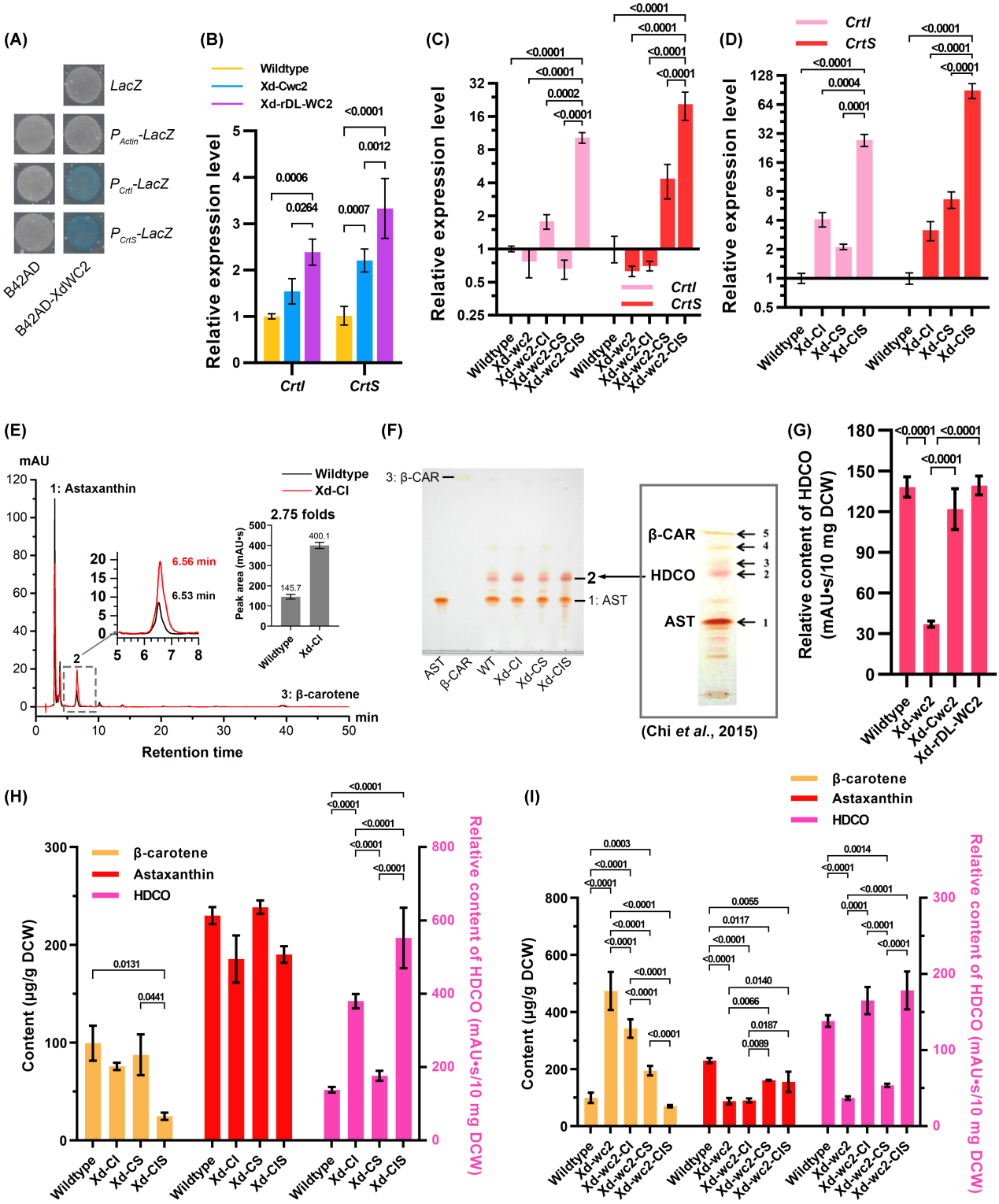

Identification of WC complex

In *N. crassa*, the GATA transcription factor WC2 combines WC1 to form the heterodimer WCC through PAS domains to regulate gene expression (Cheng et al., 2002; Linden & Macino, 1997; Schmidhauser et al., 1994). We analysed the XdWC1 protein (GenBank No. CDZ96450.1) in *X. dendrorhous* in this study. Structure analysis showed that XdWC1 had no DNA-binding domain, indicating that it was not a transcriptional repressor, unlike the WC1 in *N. crassa* (Ballario et al., 1996; Brenna & Talora, 2019) (Figure 7A). The expression of *XdWC1* did not change significantly in the transcriptomic analysis. Disruption of *XdWC1* resulted in a 1.8-fold increase in β-carotene content to 160 μg/g along with a decrease of astaxanthin by 64% (50.9 vs. 142 μg/g) and a reduction of HDCO by

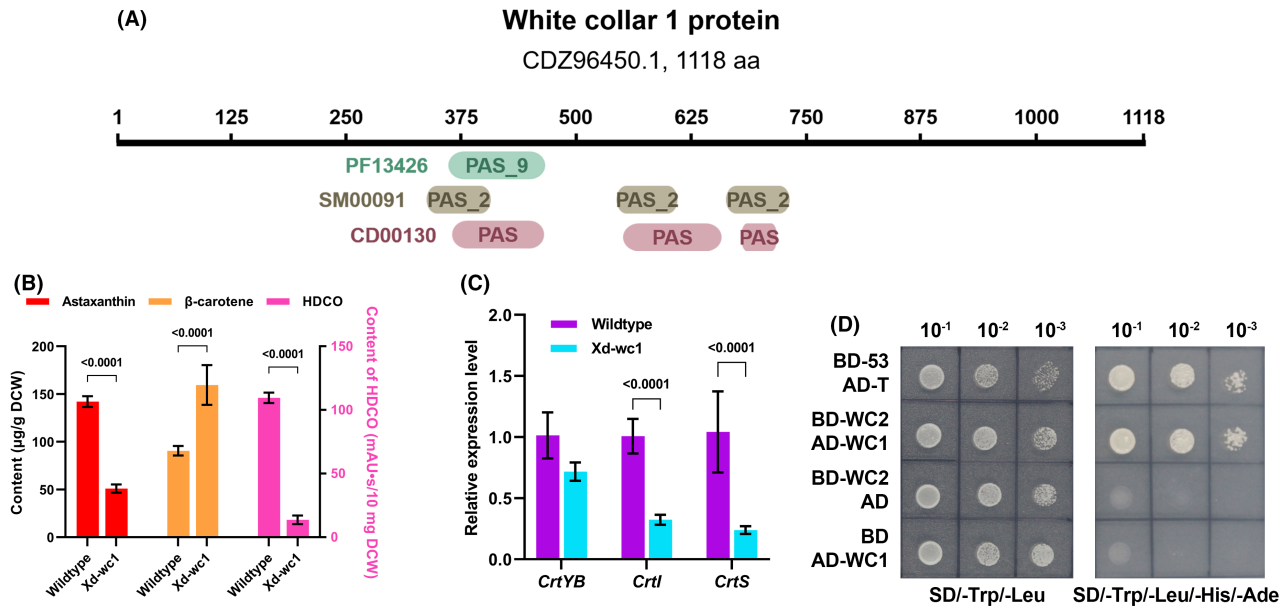

FIGURE 7 Functional analysis of XdWC1. (A) Structure analysis of XdWC1 identifying functional domains. (B) Disruption of *XdWC1* affects the production of astaxanthin, β-carotene and HDCO. Wildtype, the CBS 6938 strain; Xd-wc1, the *XdWC1*-disrupted strain. (C) The expression of *CrtYB*, *CrtI* and *CrtS* assayed by qRT-PCR in the wild-type strain CBS 6938 and Xd-wc1 when cultivated for 48 h. (D) Detection of the interaction between XdWC1 and XdWC2 by the Y2H assay. BD-53 and AD-T denote the positive control plasmids pGBKT7-53 and pGADT7-T, respectively. BD-WC2/AD and BD/AD-WC1 denote the negative controls. Cell suspension was diluted and dripped on the auxotrophic plates.

88%, respectively (Figure 7B). The expression levels of *CrtI* and *CrtS* decreased significantly when *XdWC1* was disrupted (Figure 7C). These results achieved in *XdWC1*-disrupted strain were similar to those in *XdWC2*-disrupted strain (Figure 4A and Figure 5G), suggesting that XdWC1 and XdWC2 combined to form WCC. We then performed the Y2H assay and the result confirmed that XdWC2 interacted with XdWC1 (Figure 7D). These findings indicated that XdWC2 regulates carotenoid biosynthesis by forming WCC with XdWC1 in *X. dendrorhous*.

DISCUSSION

This study identified a WC2 transcription factor XdWC2 and verified the interaction of XdWC2 with promoters of *CrtI* and *CrtS* in *X. dendrorhous*. WC2 has been extensively recognized in fungi, such as *Neurospora crassa*, *Blakeslea trispora*, *Pleurotus ostreatus* and *Metarhizium robertsii* (Corrochano, 2019; Ge et al., 2021; Peng et al., 2021; Qi et al., 2020). WC2 and WC1 combine to form WCC by PAS domains to regulate gene expression (Cheng et al., 2002). In *N. crassa*, the WCC is a key heterodimer regulator of the circadian oscillator and a blue-light receptor that mediates the expression of carotenogenic genes including GGPP synthase gene (*al-3*), phytoene synthase gene (*al-2*) and phytoene desaturase gene (*al-1*) (Linden & Macino, 1997; Schmidhauser et al., 1994). This study found that the interaction between XdWC2 and XdWC1 regulated the expression of *CrtI* (the counterpart of *al-1*), similar to the WC2 in *N. crassa*. Yet, transcriptomic analysis indicated that XdWC2 did not affect the expression of *XdWC1*, *CrtE* (the counterpart of *al-3*) and *CrtYB* (the counterpart of *al-2*), in contrast to the function of WC2 in *N. crassa*. Additionally, XdWC2 regulated the expression of the astaxanthin synthase gene *CrtS*, while *N. crassa* cannot synthesize astaxanthin. In *X. dendrorhous*, the sterol regulatory element-binding protein Sre1 directly regulates carotenogenic genes *CrtE* and *CrtR* in addition to genes related to ergosterol biosynthesis and the mevalonate pathway (Gómez et al., 2020). Both XdWC2 and Sre1 are transcription factors. XdWC2 regulates carotenogenic genes *CrtI* and *CrtS*, while Sre1 regulates carotenogenic genes *CrtE* and *CrtR*. It is interesting to further investigate the correlation between XdWC2 and Sre1 in regulating carotenoid biosynthesis in *X. dendrorhous*.

Light stimulates the biosynthesis of carotenoids in plants (Llorente et al., 2017), whereas light is not necessary for the biosynthesis of astaxanthin in *X. dendrorhous* although several studies reported that light can improve astaxanthin production, especially the blue light (Flores-Cotera et al., 2021; Meyer & Du Preez, 1994; Vázquez, 2001). In this study, we found that regulation of the expression of genes *CrtI* and *CrtS* by XdWC2 is light-independent according to the qRT-PCR analysis and the Y1H assay using cultures in darkness. In contrast to the WCC in *X. dendrorhous*, the WCC in *N. crassa* needs white light to activate to

regulate gene transcription (Linden & Macino, 1997; Schmidhauser et al., 1994). The WC1 of *N. crassa* represses gene expression in darkness through a GATA zinc-finger domain combining with promoters (Brenna & Talora, 2019), while the WC1 of *X. dendrorhous* has no GATA zinc-finger domains. These data showed the unique aspect of the metabolic regulation of astaxanthin synthesis in *X. dendrorhous*. The optimal temperature for the growth of *X. dendrorhous* is at 18–22°C and higher temperature over 22°C often decreases astaxanthin production in *X. dendrorhous* (Ducrey Sanpietro & Kula, 1998; Liu et al., 2018; Miao et al., 2021). The carbon and nitrogen concentrations in culture medium also strongly affect astaxanthin production by *X. dendrorhous* (Pan et al., 2017; Ramirez et al., 2001). Addition of glutamate in medium increases the expression of *CrtR*, *CrtI* and *CrtS* in *X. dendrorhous* (Wang et al., 2019). Since WCC is light-independent in *X. dendrorhous*, correlations between WCC and temperature and nutrition are interesting and remain to be investigated.

This study also found that overexpression of genes *XdWC2* or *CrtS* in the wild-type strain did not significantly modify the carotenoid profile. CrtS needs the auxiliary CrtR to convert β-carotene to astaxanthin. A previous study reported that the levels of *CrtR* mRNA remained constant along a five-days culture (Alcaíno et al., 2008). In this study, the transcriptomic analysis did not show obvious change in the expression of *CrtR*. These findings exhibited the rigidity of *CrtR* expression that is not closely related to the expression of *CrtS*. Taken together, CrtS may be regulated at translational or post-translational levels in addition to being regulated by *XdWC2* at the transcriptional level. CrtI is a bifunctional enzyme with activities of both phytoene desaturation and γ-carotene desaturation. Overexpression of *CrtI* in both the wild-type strain and the *XdWC2*-disrupted strain apparently improved the production of monocyclic carotenoid HDCO rather than β-carotene and astaxanthin, consistent to a previous study (Barbachano-Torres et al., 2014). Since the structures of phytoene and γ-carotene differ in terminals, it is probable to make CrtI mutants that have substrate specificity towards phytoene to improve astaxanthin production by protein engineering.

In summary, this study identified a GATA transcription factor XdWC2 in *X. dendrorhous* and confirmed that XdWC2 combines with XdWC1 forming the WC complex to regulate carotenogenic genes *CrtI* and *CrtS*. The findings presented here provides the foundation for further understanding the global regulation of astaxanthin biosynthesis and guides the construction of astaxanthin over-producing strains.

ACKNOWLEDGEMENTS

The authors thank Ms. Yixuan Fan in Qingdao Institute of Bioenergy and Bioprocess Technology for helping to edit the manuscript.

FUNDING INFORMATION

This study was supported by the Natural Science Foundation of China (51861145103 and 31670054), the National key Research and Development Program of China (2018YFE0107200) and the key grant from Shandong Energy Institute (SEI I202136).

CONFLICT OF INTEREST

The authors declare that they have no competing interests.

DATA AVAILABILITY STATEMENT

Authors have uploaded the genome resequencing and RNA sequencing data to NCBI and these data are included in the Experimental procedures in this article. The link of the genome resequencing data is https://www.ncbi.nlm.nih.gov/bioproject/PRJNA751450 and the RNA sequencing data is https://www.ncbi.nlm.nih.gov/bioproject/PRJNA752711. The datas supporting the results of this article are included within the article and supplementary table.

ORCID

Shi'an Wang https://orcid.org/0000-0001-8323-4344

REFERENCES

Alcaíno, J., Barahona, S., Carmona, M., Lozano, C., Marcoleta, A., Niklitschek, M. et al. (2008) Cloning of the cytochrome p450 reductase (*crtR*) gene and its involvement in the astaxanthin biosynthesis of *Xanthophyllomyces dendrorhous*. *BMC Microbiology*, 8, 169.

Álvarez, V., Rodríguez-Sáiz, M., de la Fuente, J.L., Gudiña, E.J., Godio, R.P., Martín, J.F. et al. (2006) The crtS gene of *Xanthophyllomyces dendrorhous* encodes a novel cytochrome-P450 hydroxylase involved in the conversion of β-carotene into astaxanthin and other xanthophylls. *Fungal Genetics and Biology*, 43, 261–272.

Ambati, R.R., Phang, S.M., Ravi, S. & Aswathanarayana, R.G. (2014) Astaxanthin: sources, extraction, stability, biological activities and its commercial applications—a review. *Marine Drugs*, 12, 128–152.

Bailey, T.L., Boden, M., Buske, F.A., Frith, M., Grant, C.E., Clementi, L. et al. (2009) MEME Suite: tools for motif discovery and searching. *Nucleic Acids Research*, 37, W202–W208.

Ballario, P., Vittorioso, P., Magrelli, A., Talora, C., Cabibbo, A. & Macino, G. (1996) White collar-1, a central regulator of blue light responses in *Neurospora*, is a zinc finger protein. *The EMBO Journal*, 15, 1650–1657.

Barbachano-Torres, A., Castelblanco-Matiz, L.M., Ramos-Valdivia, A.C., Cerda-García-Rojas, C.M., Salgado, L.M., Flores-Ortiz, C.M. et al. (2014) Analysis of proteomic changes in colored mutants of *Xanthophyllomyces dendrorhous* (*Phaffia rhodozyma*). *Archives of Microbiology*, 196, 411–421.

Barredo, J.L., García-Estrada, C., Kosalkova, K. & Barreiro, C. (2017) Biosynthesis of astaxanthin as a main carotenoid in the heterobasidiomycetous yeast *Xanthophyllomyces dendrorhous*. *Journal of Fungi (Basel)*, 3, 44.

Barreiro, C. & Barredo, J.L. (2018) Carotenoids production: a healthy and profitable industry. *Methods in Molecular Biology*, 1852, 45–55.

Basiony, M., Ouyang, L.M., Wang, D.N., Yu, J.M., Zhou, L.M., Zhu, M.H. et al. (2022) Optimization of microbial cell factories for astaxanthin production: biosynthesis and regulations,

engineering strategies and fermentation optimization strategies. *Synthetic and Systems Biotechnology*, 7, 689–704.

Blum, M., Chang, H.Y., Chuguransky, S., Grego, T., Kandasaamy, S., Mitchell, A. et al. (2021) The InterPro protein families and domains database: 20 years on. *Nucleic Acids Research*, 49, D344–D354.

Bogacz-Radomska, L. & Harasym, J. (2018) β-Carotene—properties and production methods. *Food Quality and Safety*, 2, 69–74.

Brenna, A. & Talora, C. (2019) WC-1 and the proximal GATA sequence mediate a *cis–/trans*-acting repressive regulation of light-dependent gene transcription in the dark. *International Journal of Molecular Sciences*, 20, 2854.

Chen, S.F., Zhou, Y.Q., Chen, Y.R. & Gu, J. (2018) Fastp: an ultra-fast all-in-one FASTQ preprocessor. *Bioinformatics*, 34, i884–i890.

Chen, C.J., Chen, H., Zhang, Y., Thomas, H.R., Frank, M.H., He, Y.H. et al. (2020) TBtools: an integrative toolkit developed for interactive analyses of big biological data. *Molecular Plant*, 13, 1194–1202.

Cheng, P., Yang, Y.H., Gardner Kevin, H. & Liu, Y. (2002) PAS domain-mediated WC-1/WC-2 interaction is essential for maintaining the steady-state level of WC-1 and the function of both proteins in circadian clock and light responses of *Neurospora*. *Molecular and Cellular Biology*, 22, 517–524.

Chi, S., He, Y.F., Ren, J., Su, Q., Liu, X.C., Chen, Z. et al. (2015) Overexpression of a bifunctional enzyme, CrtS, enhances astaxanthin synthesis through two pathways in *Phaffia rhodozyma*. *Microbial Cell Factories*, 14, 90.

Corrochano, L.M. (2019) Light in the fungal world: from photoreception to gene transcription and beyond. *Annual Review of Genetics*, 53, 149–170.

Ducrey Sanpietro, L.M. & Kula, M.R. (1998) Studies of astaxanthin biosynthesis in *Xanthophyllomyces dendrorhous* (*Phaffia rhodozyma*). Effect of inhibitors and low temperature. *Yeast (Chichester, England)*, 14, 1007–1016.

Fakhri, S., Abbaszadeh, F., Dargahi, L. & Jorjani, M. (2018) Astaxanthin: a mechanistic review on its biological activities and health benefits. *Pharmacological Research*, 136, 1–20.

Flores-Cotera, L.B., Chávez-Cabrera, C., Martínez-Cárdenas, A., Sánchez, S. & García-Flores, O.U. (2021) Deciphering the mechanism by which the yeast *Phaffia rhodozyma* responds adaptively to environmental, nutritional, and genetic cues. *Journal of Industrial Microbiology & Biotechnology*, 48, kuab048.

Ge, X., Yuan, Y.T., Li, R.Q., Zhang, X.M. & Xin, Q. (2021) Structure prediction and function characterization of WC-2 proteins in *Blakeslea trispora*. *International Microbiology*, 24, 427–439.

Gómez, M., Campusano, S., Gutiérrez, M.S., Sepúlveda, D., Barahona, S., Baeza, M. et al. (2020) Sterol regulatory element-binding protein Sre1 regulates carotenogenesis in the red yeast *Xanthophyllomyces dendrorhous*. *Journal of Lipid Research*, 61, 1658–1674.

Gómez, M., Baeza, M., Cifuentes, V. & Alcaíno, J. (2021) The SREBP (Sterol Regulatory Element-Binding Protein) pathway: a regulatory bridge between carotenogenesis and sterol biosynthesis in the carotenogenic yeast *Xanthophyllomyces dendrorhous*. *Biological Research*, 54, 34.

Grand View Research Inc. (2021) Astaxanthin market size, share & trends analysis report by product (oil, softgel, liquid), by source (natural, synthetic), by application (aquaculture & animal feed, nutraceuticals), by region, and segment forecasts, 2021–2028. Grand View Research.

Kim, D., Langmead, B. & Salzberg, S.L. (2015) HISAT: a fast spliced aligner with low memory requirements. *Nature Methods*, 12, 357–360.

Larkin, M.A., Blackshields, G., Brown, N.P., Chenna, R., McGettigan, P.A., McWilliam, H. et al. (2007) Clustal W and Clustal X version 2.0. *Bioinformatics*, 23, 2947–2948.

Li, H. & Durbin, R. (2009) Fast and accurate short read alignment with Burrows-Wheeler transform. *Bioinformatics*, 25, 1754–1760.

Li, H., Handsaker, B., Wysoker, A., Fennell, T., Ruan, J., Homer, N. et al. (2009) The Sequence Alignment/Map format and SAMtools. *Bioinformatics*, 25, 2078–2079.

Liang, X.Q., Ma, C.C., Yan, X.J., Liu, X.B. & Liu, F.G. (2019) Advances in research on bioactivity, metabolism, stability and delivery systems of lycopene. *Trends in Food Science and Technology*, 93, 185–196.

Lin, R.C., Ding, L., Casola, C., Ripoll Daniel, R., Feschotte, C. & Wang, H.Y. (2007) Transposase-derived transcription factors regulate light signaling in *Arabidopsis*. *Science*, 318, 1302–1305.

Linden, H. & Macino, G. (1997) White collar 2, a partner in blue-light signal transduction, controlling expression of light-regulated genes in *Neurospora crassa*. *The EMBO Journal*, 16, 98–109.

Liu, S.W., Liu, B.N., Wang, H., Xiao, S., Li, Y. & Wang, J.H. (2018) Production of astaxanthin at moderate temperature in *Xanthophyllomyces dendrorhous* using a two-step process. *Engineering in Life Sciences*, 18, 706–710.

Livak, K.J. & Schmittgen, T.D. (2001) Analysis of relative gene expression data using real-time quantitative PCR and the $2^{-\Delta\Delta CT}$ method. *Methods*, 25, 402–408.

Llorente, B., Martinez-Garcia, J.F., Stange, C. & Rodriguez-Concepcion, M. (2017) Illuminating colors: regulation of carotenoid biosynthesis and accumulation by light. *Current Opinion in Plant Biology*, 37, 49–55.

Marcoleta, A., Niklitschek, M., Wozniak, A., Lozano, C., Alcaíno, J., Baeza, M. et al. (2011) Glucose and ethanol-dependent transcriptional regulation of the astaxanthin biosynthesis pathway in *Xanthophyllomyces dendrorhous*. *BMC Microbiology*, 11, 190.

Martínez-Cámara, S., Ibañez, A., Rubio, S., Barreiro, C. & Barredo, J.L. (2021) Main carotenoids produced by microorganisms. *Encyclopedia*, 1, 1223–1245.

McKenna, A., Hanna, M., Banks, E., Sivachenko, A., Cibulskis, K., Kernytsky, A. et al. (2010) The Genome Analysis Toolkit: a MapReduce framework for analyzing next-generation DNA sequencing data. *Genome Research*, 20, 1297–1303.

Meng, D., Li, C.L., Park, H.J., González, J., Wang, J.Y., Dandekar, A.M. et al. (2018) Sorbitol modulates resistance to *Alternaria alternata* by regulating the expression of an *NLR* resistance gene in apple. *Plant Cell*, 30, 1562–1581.

Meyer, P.S. & Du Preez, J.C. (1994) Photo-regulated astaxanthin production by *Phaffia rhodozyma* mutants. *Systematic and Applied Microbiology*, 17, 24–31.

Miao, L.L., Chi, S., Hou, T.T., Liu, Z.P. & Li, Y. (2021) The damage and tolerance mechanisms of *Phaffia rhodozyma* mutant strain MK19 grown at 28°C. *Microbial Cell Factories*, 20, 5.

Mohamadnia, S., Tavakoli, O., Faramarzi, M.A. & Shamsollahi, Z. (2020) Production of fucoxanthin by the microalga *Tisochrysis lutea*: a review of recent developments. *Aquaculture*, 516, 734637.

Moretti, V.M., Mentasti, T., Bellagamba, F., Luzzana, U., Caprino, F., Turchini, G.M. et al. (2006) Determination of astaxanthin stereoisomers and colour attributes in flesh of rainbow trout (*Oncorhynchus mykiss*) as a tool to distinguish the dietary pigmentation source. *Food Additives and Contaminants*, 23, 1056–1063.

Mussagy, C.U., Pereira, J.F.B., Dufossé, L., Raghavan, V., Santos-Ebinuma, V.C. & Pessoa, A., Jr. (2021) Advances and trends in biotechnological production of natural astaxanthin by *Phaffia rhodozyma* yeast. *Critical Reviews in Food Science and Nutrition*, 26, 1–15.

Naguib, Y.M.A. (2000) Antioxidant activities of astaxanthin and related carotenoids. *Journal of Agricultural and Food Chemistry*, 48, 1150–1154.

Niklitschek, M., Baeza, M., Fernández-Lobato, M. & Cifuentes, V. (2012) Generation of astaxanthin mutants in *Xanthophyllomyces*

dendrorhous using a double recombination method based on hygromycin resistance. In: Barredo, J.L. (Ed.) *Microbial carotenoids from fungi: methods and protocols*. Totowa, NJ: Humana Press, pp. 219–234.

Pan, X.S., Wang, B.B., Gerken, H.G., Lu, Y.H. & Ling, X.Q. (2017) Proteomic analysis of astaxanthin biosynthesis in *Xanthophyllomyces dendrorhous* in response to low carbon levels. *Bioprocess and Biosystems Engineering*, 40, 1091–1100.

Park, J.S., Kim, H.J., Kim, S.O., Kong, S.H., Park, J.J., Kim, S.R. et al. (2006) A comparative genome-wide analysis of GATA transcription factors in fungi. *Genomics and Informatics*, 4, 147–160.

Peng, H., Guo, C.T., Tong, S.M., Ying, S.H. & Feng, M.G. (2021) Two white collar proteins protect fungal cells from solar UV damage by their interactions with two photolyases in *Metarhizium robertsii*. *Environmental Microbiology*, 23, 4925–4938.

Perrière, G. & Gouy, M. (1996) WWW-Query: an on-line retrieval system for biological sequence banks. *Biochimie*, 78, 364–369.

Qi, Y.C., Sun, X.K., Ma, L., Wen, Q., Qiu, L.Y. & Shen, J.W. (2020) Identification of two *Pleurotus ostreatus* blue light receptor genes (PoWC-1 and PoWC-2) and *in vivo* confirmation of complex PoWC-12 formation through yeast two hybrid system. *Fungal Biology*, 124, 8–14.

Ramirez, J., Gutierrez, H. & Gschaedler, A. (2001) Optimization of astaxanthin production by *Phaffia rhodozyma* through factorial design and response surface methodology. *Journal of Biotechnology*, 88, 259–268.

Roberts, A., Trapnell, C., Donaghey, J., Rinn, J.L. & Pachter, L. (2011) Improving RNA-Seq expression estimates by correcting for fragment bias. *Genome Biology*, 12, R22.

Rodríguez-Sáiz, M., de la Fuente, J.L. & Barredo, J.L. (2010) *Xanthophyllomyces dendrorhous* for the industrial production of astaxanthin. *Applied Microbiology and Biotechnology*, 88, 645–658.

Rüfer, C., Moeseneder, J., Briviba, K., Rechkemmer, G. & Bub, A. (2008) Bioavailability of astaxanthin stereoisomers from wild (*Oncorhynchus* spp.) and aquacultured (*Salmo salar*) salmon in healthy men: a randomised, double-blind study. *The British Journal of Nutrition*, 99, 1048–1054.

Schaub, P., Yu, Q.J., Gemmecker, S., Poussin-Courmontagne, P., Mailliot, J., McEwen, A.G. et al. (2012) On the atructure and function of the phytoene desaturase CRTI from *Pantoea ananatis*, a membrane-peripheral and FAD-dependent oxidase/isomerase. *PLoS One*, 7, e39550.

Schmidhauser, T.J., Lauter, F.R., Schumacher, M., Zhou, W.B., Russo, V.E.A. & Yanofsky, C. (1994) Characterization of *al-2*, the phytoene synthase gene of *Neurospora crassa*. cloning, sequence analysis, and photoregulation. *The Journal of Biological Chemistry*, 269, 12060–12066.

Shimidzu, N., Goto, M. & Miki, W. (1996) Carotenoids as singlet oxygen quenchers in marine organisms. *Fisheries Science*, 62, 134–137.

Stachowiak, B. & Szulc, P. (2021) Astaxanthin for the food industry. *Molecules*, 26, 2666.

Torres-Haro, A., Verdín, J., Kirchmayr, M.R. & Arellano-Plaza, M. (2021) Metabolic engineering for high yield synthesis of astaxanthin in *Xanthophyllomyces dendrorhous*. *Microbial Cell Factories*, 20, 175.

Vázquez, M. (2001) Effect of the light on carotenoid profiles of *Xanthophyllomyces dendrorhous* strains (formerly *Phaffia rhodozyma*). *Food Technology and Biotechnology*, 39, 123–128.

Wang, B.B., Pan, X.S., Jia, J., Xiong, W.D., Manirafasha, E., Ling, X.Q. et al. (2019) Strategy and regulatory mechanisms of glutamate feeding to enhance astaxanthin yield in *Xanthophyllomyces dendrorhous*. *Enzyme and Microbial Technology*, 125, 45–52.

Wery, J., Verdoes, J.C. & van Ooyen, A.J.J. (1998) Efficient transformation of the astaxanthin-producing yeast *Phaffia rhodozyma*. *Biotechnology Techniques*, 12, 399–405.

Wozniak, A., Lozano, C., Barahona, S., Niklitschek, M., Marcoleta, A., Alcaíno, J. et al. (2011) Differential carotenoid production and gene expression in *Xanthophyllomyces dendrorhous* grown in a nonfermentable carbon source. *FEMS Yeast Research*, 11, 252–262.

Yang, M.Z., Derbyshire, M.K., Yamashita, R.A. & Marchler-Bauer, A. (2020a) NCBI's conserved domain database and tools for protein domain analysis. *Current Protocols in Bioinformatics*, 69, e90.

Yang, J.J., Zhang, G.Q., An, J., Li, Q.X., Chen, Y.H., Zhao, X.Y. et al. (2020b) Expansin gene *TaEXPA2* positively regulates drought tolerance in transgenic wheat (*Triticum aestivum* L.). *Plant Science*, 298, 110596.

Yu, M.N., Yu, J.J., Cao, H.J., Yong, M.L. & Liu, Y.F. (2019) Genome-wide identification and analysis of the GATA transcription factor gene family in *Ustilaginoidea virens*. *Genome*, 62, 807–816.

Zafar, J., Aqeel, A., Shah, F.I., Ehsan, N., Gohar, U.F., Moga, M.A. et al. (2021) Biochemical and immunological implications of lutein and zeaxanthin. *International Journal of Molecular Sciences*, 22, 10910.

Zhang, N., Li, J.X., Li, F.L. & Wang, S.A. (2019) Selectable marker recycling in the nonconventional yeast *Xanthophyllomyces dendrorhous* by transient expression of Cre on a genetically unstable vector. *Applied Microbiology and Biotechnology*, 103, 963–971.

SUPPORTING INFORMATION

Additional supporting information can be found online in the Supporting Information section at the end of this article.

How to cite this article: Huang, R., Ding, R., Liu, Y., Li, F., Zhang, Z. & Wang, S. (2022) GATA transcription factor WC2 regulates the biosynthesis of astaxanthin in yeast *Xanthophyllomyces dendrorhous*. *Microbial Biotechnology*, 15, 2578–2593. Available from: https://doi.org/10.1111/1751-7915.14115